Journal of Traditional and Complementary Medicine 12 (2022) 162–171

Contents lists available at ScienceDirect

Journal of Traditional and Complementary Medicine

journal homepage: http://www.elsevier.com/locate/jtcme

Mechanistic insights into the antimycobacterial action of unani formulation, Qurs Sartan Kafoori

Saif Hameed [a], Sandeep Hans [a], Shiv Nandan [b], Zeeshan Fatima [a, *]

[a] Amity Institute of Biotechnology, Amity University Haryana, Manesar, Gurugram, 122413, India
[b] Amity Lipidomics Research Facility, Amity University Haryana, Manesar, Gurugram, 122413, India

ARTICLE INFO

Article history:
Received 23 February 2021
Received in revised form
28 July 2021
Accepted 29 July 2021
Available online 30 July 2021

Keywords:
Mycobacterium
unani drug
Cell membrane
Lipidomics
Biofilm
ROS

ABSTRACT

Background and aim: Tuberculosis (TBC) is a deadly disease and major health issue in the world. Emergence of drug resistant strains further worsens the efficiency of available anti-TBC drugs. Natural compounds and particularly traditional medicines such as Unani drugs are one of the promising alternatives that have been widely used nowadays. This study aims to evaluate the efficacy of unani drug Qurs-e-Sartan Kafoori (QSK) on *Mycobacterium tuberculosis* (MTB).

Experimental procedures: Drug susceptibilities were estimated by broth microdilution assay. Cell surface integrity was assessed by ZN staining, colony morphology and nitrocefin hydrolysis. Biofilms were visualized by crystal violet staining and measurement of metabolic activity and biomass. Lipidomics analysis was performed using mass spectrometry. Host pathogen interaction studies were accomplished using THP-1 cell lines to estimate cytokines by ELISA kit, apoptosis and ROS by flow cytometry.

Results: QSK enhanced the susceptibilities of isoniazid and rifampicin and impaired membrane homeostasis as depicted by altered cell surface properties and enhanced membrane permeability. In addition, virulence factor, biofilm formation was considerably reduced in presence of QSK. Lipidomic analysis revealed extensive lipid remodeling. Furthermore, we used a THP-1 cell line model, and investigated the immunomodulatory effect by estimating cytokine profile and found change in expressions of TNF-α, IL-6 and IL-10. Additionally, we uncover reduced THP-1 apoptosis and enhanced ROS production in presence of QSK.

Conclusion: Together, this study validates the potential of unani formulation (QSK) with its mechanism of action and attempts to highlight its significance in MDR reversal.

1. Introduction

Infectious diseases are the main cause of human death worldwide and Tuberculosis (TBC) which is an ancient disease has affected mankind for more than 4,000 years.[1] TB remains a leading cause of morbidity and mortality in developing countries. The estimated number of infections by *Mycobacterium tuberculosis* (MTB), causative agent of TBC is one third of the world population with 8–9 million new TBC cases each year and about 1–2 million yearly deaths.[2] According to report of WHO in 2018, the 30 high TBC burden countries accounted for 87% of new TBC cases among which 8 countries contributed for two thirds of the total, with India leading the count. The report also described a total of 1.5 million people who died from TBC in 2018 and 10 million people fell ill with TBC worldwide which included 5.7 million men, 3.2 million women and 1.1 million children (including 251,000 people with HIV).[3] Worldwide, TBC is one of the top 10 causes of death and the leading cause from a single infectious agent (above HIV/AIDS).[4] The situation get worsen with the emergence of multidrug-resistant TBC (MDR-TBC) which is a public health crisis and a health security threat. WHO estimated around 484,000 new cases with resistance to rifampicin, the most effective first-line drug of which 78% had MDR-TBC. The MDR-TBC burden largely falls on 3 countries India, China and the Russian Federation which together accounts

Abbreviations: Qurs sartan kafoori, (QSK); Isoniazid, (INH); Rifampicin, (RIF); Streptomycin, (STP); Ethambutol, (EMB); Reactive oxygen species, (ROS); fatty acid, (FA); glycerolipids, (GL); glycerophospholipids, (GPL).

* Corresponding author.
E-mail address: drzeeshanfatima@gmail.com (Z. Fatima).

Peer review under responsibility of The Center for Food and Biomolecules, National Taiwan University.

https://doi.org/10.1016/j.jtcme.2021.07.009

for half of the global cases.[5] About 6.2% of MDR-TBC cases had extensively drug-resistant TB (XDR-TBC) in 2018 (Ministry of Health and Family Welfare 2018).[5] Therefore it is necessary to develop novel, effective and affordable anti-TBC drugs to combat MDR.

Natural compounds and particularly traditional medicines are one of the alternative and important emerging sources with lesser side effect that have been widely used nowadays. Furthermore, in the same context, adopting the management or principles of Unani system would be beneficial in health and disease. Some ancient literature has numerous citation of pulmonary TBC. Unani physicians used the term "Sil and Dique to describe TBC.[6] The primary symptom of TB is chronic cough. In unani system of medicine chronic cough has successful treatment with Qurs-e-Sartan Kafoori.[7] Qurs-e-Sartan Kafoori (QSK)- is composed of 19 components of which majority are from medicinal plants. The botanical names of few ingredients of QSK are: *Cinnamomum camphora Nees*, *Santalum album Linn*., *Pterocarpus Santalinus Linn.f*., *Lactuca Sativa Linn*., *Acacia arabica Wild*., *Portulaca oleracea Linn*. & *Cucurbita maxima Duch*., *Cucumis Sativus Linn*., *Cucumis utilissimus Roxb*., *Scilla SArrata Crab*.[8] It is a mixture of crystals Kafoor, Shell of Sartan Nahri (Crab) and several seed & root extracts and exudates. It is an effective remedy to treat chronic bronchitis & cough. The medicinal values of these unani formulations are at primitive stage only against TBC. The mechanistic approach of these unani drugs are yet to be elucidated. Considering the importance of Unani Drug (QSK) in other pathologies, this study evaluates the combinatorial effect of QSK against MTB, along with the mode of action and immunomodulatory effect and attempts to highlight its significance in MDR reversal.

2. Material and methods

2.1. Material

All Media chemicals Middlebrook 7H9 broth, Middlebrook 7H10 agar, albumin/dextrose/catalase (ADC), oleic acid/albumin/dextrose/catalase (OADC) supplements were purchased from BD Biosciences (USA). Tween-80, Roswell Park Memorial Institute Medium (RPMI), Phorbol 12-myristate 13-acetate (PMA), Amikacin, Fetal bovine serum (FBS), Isoniazid (INH), Rifampicin (RIF), Streptomycin (STP) and DCFDA (dichlorodihydro-fluorescein diacetate) were obtained from Sigma Chemical Co. (St.Louis, MO, USA). Chloroform, hexane (C6H14), diethyl ether ($(C_2H_5)_2O$), sulfuric acid (H_2SO_4), and iodine (I), Methanol (CH_3OH), Triton X-100, crystal violet (CV), peptone, p-dimethyl aminobenzaldehyde, ethambutol (EMB) were purchased from Himedia (Mumbai, India). Dimethyl sulfoxide (DMSO), Potassium chloride (KCl), Sodium chloride (NaCl), di-Sodium Hydrogen Orthophosphate (Na_2HPO_4), Potassium Di-hydrogen Orthophosphate (KH_2PO_4), Glycerol, magnesium chloride ($MgCl_2$), calcium chloride ($CaCl_2$), were obtained from Fischer Scientific. Agarose was purchased from CDH India.

2.2. Bacterial strains used in this study

Bacterial strain used in this study was *Mycobacterium tuberculosis* $H_{37}Rv$ obtained from Vallabhbhai Patel Chest Institute, Delhi.

2.2.1. Culture conditions

Mycobacterium tuberculosis $H_{37}Rv$ was grown in Middlebrook 7H9 broth supplemented with 0.05% Tween-80 and 0.2% glycerol and for solid media Middlebrook 7H10 agar media supplemented with 10% (v/v) OADC (BD Biosciences) was used followed by incubation for 48 h at 37 °C. Stock cultures of log-phase cells were maintained in 30% glycerol and stored at −80 °C.

2.2.2. QSK and Dose dependent growth response

The unani formulation Qurs-Sartan Kafoori (QSK) was obtained commercially from Unani pharmacy. Briefly, about five tablets were crushed in mortar and pestle and suspended overnight in 20 ml chloroform. The suspension was filtered with muslin cloth and dried at 45 °C on magnetic stirrer with addition of 10 ml of autoclave water. We used dose-dependent method to evaluate growth inhibition in the presence of QSK. Briefly, MTB cells were inoculated with various concentrations of QSK in Sauton media and incubated at 37 °C for 24h. Post incubation, absorbance of the samples was observed at OD_{600} nm. We choose 12 mg/ml QSK for all biochemical experiments that was enough to show partial inhibitory effect on MTB (Fig. S1).

2.3. Drug potentiation assay

Broth microdilution assay was performed as described previously.[9,10] Two hundred microliters of sterile media was added to all left outer-perimeter wells of the plates. The plates were prepared by dispensing the serially diluted antibiotics (INH, EMB, RIF and STP) in addition with QSK. Aliquots of 0.1 ml of inoculums adjusted to OD_{600} 0.1 and diluted 1:100 were transferred to each well of the 96-well plate and incubated at 37 °C. The inoculated plates were sealed in plastic bags and incubated at 37 °C for 7 days. After 7 days of incubation, 30 μL of resazurin salt was added to each well, incubated for another 2 days at 37 °C and assessed for the color development. A change from blue to pink indicates reduction of resazurin and therefore bacterial growth. The MIC was defined as the lowest drug concentration that prevented this color change.

2.4. Cell sedimentation assay

Cell Sedimentation assay was performed as described previously.[9,11] Both the control and treated cells (with QSK) at OD_{600} ~ 1.0–1.4, grown in Sauton media, were adjusted to OD_{600} ~ 1.0 and kept unshaken at 37 °C. At 3 and 22 h, the upper 1 ml was removed for measurements at OD_{590} and graph was plotted as described in figure legends.

2.5. Biofilm and biomass estimation

MTB biofilm-forming potential was qualitatively and quantitatively analyzed using the microtiter-plate method as described previously.[9,10] Briefly, MTB cultures were grown at 37 °C in Middlebrook media, followed by transfer of 100 μL of the media in each well of the 96-well plate in absence and presence of QSK. Cultures that had reached an OD_{600} of 0.1 were diluted (1:100) using Middlebrook media, and 100 μL of each diluted culture was pipetted into each well of a 96-well flat-bottom microtiter plate and incubated at 37 °C for 21days. The wells were rinsed with water and cells were fixed with 4% paraformaldehyde followed by 4hrs incubation. Then 125 μL of 0.1% solution of the crystal violet was added. Plates were incubated for 10 min, followed by washing with distilled H_2O three times. For quantitative assays of the biofilm, 200 μL of 95% ethanol was added to each crystal violet-stained well, and plates were incubated for 10 min at room temperature followed by transfer of 125 μL of the crystal violet/ethanol solution from each well to a separate well. The OD_{600} was measured using a spectrophotometer. For qualitative assay, MTB bioflms were formed in the absence (control) and presence of QSK, at OD_{600} of 1.0 and incubated for 21days at 37°C in 12-well plate containing coverslips. The pre-weight coverslips were rinsed with distilled water and the dry weight was measured after biofilm formation by calculating the difference. 1% CV was added to each coverslip, and incubated for 10 min at room temperature. Then coverslips were rinsed with PBS

and visualized under fluorescent microscope at 40x.

2.6. Total lipid extraction and thin layer chromatography (TLC)

Cells of MTB control and in presence of QSK (12 mg/ml)were incubated at 37 °C till 12–14 days and were used for lipid extraction by modified Folch method.[10,12] Briefly, the cells were harvested at 2100×*g* for 10 min. Cells were homogenized in aqueous solution for 3 min and suspended in $CHCl_3$ and CH_3OH in ratio of (1:2). Cells were shaken well and centrifuged at 500×*g* at 4 °C for 15 min. Supernatant was transferred to another glass vial and then remaining $CHCl_3$ was added and filtered through Whatman No. 1 filter paper. The extract was then washed with 0.88% KCl to remove the non-lipid contamination. The lower dense layer of chloroform containing lipid was taken by glass Pasteur pipette in 5 ml glass vial with Teflon capping. The vials are stored at −20 °C until further analysis. Extracted lipids were then resolved by TLC using aluminum-backed silica gel plates (silica gel 60 F254; Merck). Chloroform-methanol-water (65:25:4; v/v/v) was used for developing the plates. Developed chromatogram was dried at room temperature for 2 min and then exposed to iodine fumes generated by iodine crystal balls placed in glass chamber to visualize the lipids (Fig. S2).

2.7. Ultra performance liquid chromatography electrospray ionization and mass spectrometry (UPLC-ESI–MS)

The isolated lipids from MTB cells of untreated and treated with QSK (12 mg/ml) incubated at 37 °C till 12–14 days were used to perform reverse-phase ultrahigh-pressure liquid chromatography (UHPLC, Exion LC Sciex, USA) using an Kinetex C18, 2.1 × 50 mm column (Phenomenex, USA) with a particle size of 1.7 μm column coupled to a hybrid triple quadrupole/linear ion trap mass spectrometer (4500 Q-TRAP, SCIEX, USA). The elution was done for 30 min, using mobile phase A and B, solvent A have 10% methanol and 90% buffer of ammonium acetate (5 mM) dissolved in (95:5 water and acetonitrile) and solvent B have 5% isopropanol, 10% methanol and 85% acetonitrile. The sample was introduced using an autosampler with 5 μL of sample injection volume. The data were recorded in the mass range, *m/z* 200–2000 Da in ESI ± mode and processing was performed with the Analyst software, where each chromatogram was smoothened and the background was subtracted. The analysis of the acquired data was performed by mass spectrometry-based lipid (ome) Analyzer and molecular platform (MS-LAMP) software.[11,13,14] This software is a graphical user interface (GUI) standalone programme built using Perl::Tk. It is a combination of MTB lipid database (www.mrl. colostate.edu) and lipid metabolites and pathways strategy consortium (LIPID MAPS; www.lipidmaps.org). The adduct used for analysis were $[M + H]^+$, $[M + NH_4]^+$, $[M + Na]^+$, $[M - H]^-$ and 0.5 window range was used for analysis. Further, it needs to be noted that the data herein are analyzed qualitatively only. All the experiments were performed in triplicates to ensure reproducibility and accuracy.

2.8. THP-1 macrophage infection

THP-1 cells were grown in RPMI 1640 supplemented with 10% fetal bovine serum (FBS).[15] To differentiate from monocyte to macrophage the cells were treated with 15 nM PMA for 48h and then washed three times. Cells were seeded with fresh media for 1 day to overcome the stress induction by PMA before infection. MTB cells were grown to log phase. Prior to infection, 1-ml cultures of mycobacterial strain were pelleted for 2 min, resuspended in RPMI 1640, vortexed for 2 min, and passed through syringe (26 gauge needle) for 2-3 times. To ensure an infection ratio of 10 bacilli per macrophage infecting for 4 h, followed by treatment of amikacin to kill the cells outside the macrophage. Then cells were washed with PBS and resuspended with RPMI supplemented with 10% FBS along with drug QSK. Media were changed every 2 days during an infection time of 1–7 days. To determine the numbers of CFUs, supernatants were aspirated and monolayers were washed gently with phosphate buffer solution (PBS) three times before being lysed with 0.5% Triton X-100. The lysates were serially diluted in triplicate, plated on Middlebrook 7H10 agar plates and CFUs determined.

2.9. Cytokine estimation by ELISA

Supernatants collected from infected cells for 0, 2, 4 and 6 day was collected. These were stored at −20C until tested for levels of cytokines IL-6, IL-10 and TNFα using an enzyme linked immunosorbent assay (ELISA) kit according to the manufacturer's (ABTS, Peprotech, USA) instructions.[16]

2.10. Intracellular apoptosis

Apoptosis of THP-1 cells was estimated with an Annexin-FITC staining kit (R&D Systems, Minn., and U.S.A.) as per the manufacturer's instructions and analyzed by flow cytometry.[16] Briefly, the infected THP-1 cells in presence and absence of QSK were detached with cold PBS (4 °C), pelleted at 300×*g* for 10 min and washed twice in 1 ml PBS. The reaction mixture containing Annexin-FITC was prepared in 100 μl of binding buffer as per the instruction and was added to the samples and vortexed gently. The cells with reaction mixture were incubated in the dark for 15–30 min for labeling and fixed in 4% paraformaldehyde. An additional 400 μl of binding buffer was added prior to acquisition. The labeled cells were then acquired in FACScan and analyzed by Cellquest software.

2.11. Intracellular ROS estimation

Intracellular ROS levels were measured by DCFH-DA as described previously.[17] Briefly, THP-1 cell were differentiated in culture dishes and infected with bacterial strains (MOI = 10) in the presence and absence of QSK for 30 min. Cells were then incubated with DCFH-DA (5 mM)) for 30 min at 37 °C in 5% CO2 and then washed HBSS (for DCFH-DA staining). Total intracellular levels of ROS were determined by FACS analyses of the oxidative conversion of cell-permeable DCFH-DA, using the FACS (BD, USA). .

2.12. Statistical analysis

All experiments were performed in triplicates (n = 3). The results were reported as mean ± standard deviation (SD) and analyzed using Student t-test where only $p < 0.05$ was considered as statistically significant.

3. Results

3.1. Drugs susceptibility is enhanced in response to QSK

We studied the effect of QSK on susceptibilities of known antimycobacterial drugs such as rifampicin (RIF), isoniazid (INH), ethambutol (EMB) and streptomycin (STP) (Fig. 1A). We found one fold enhanced susceptibilities of RIF and INH in presence of QSK with no change for EMB and STP (Fig. 1). For instance the MIC of RIF falls from 15.6 ng/ml to 7.8 ng/ml in presence of QSK. Similarly, MIC of INH falls from 31.25 ng/ml to 15.6 ng/ml in presence of QSK.

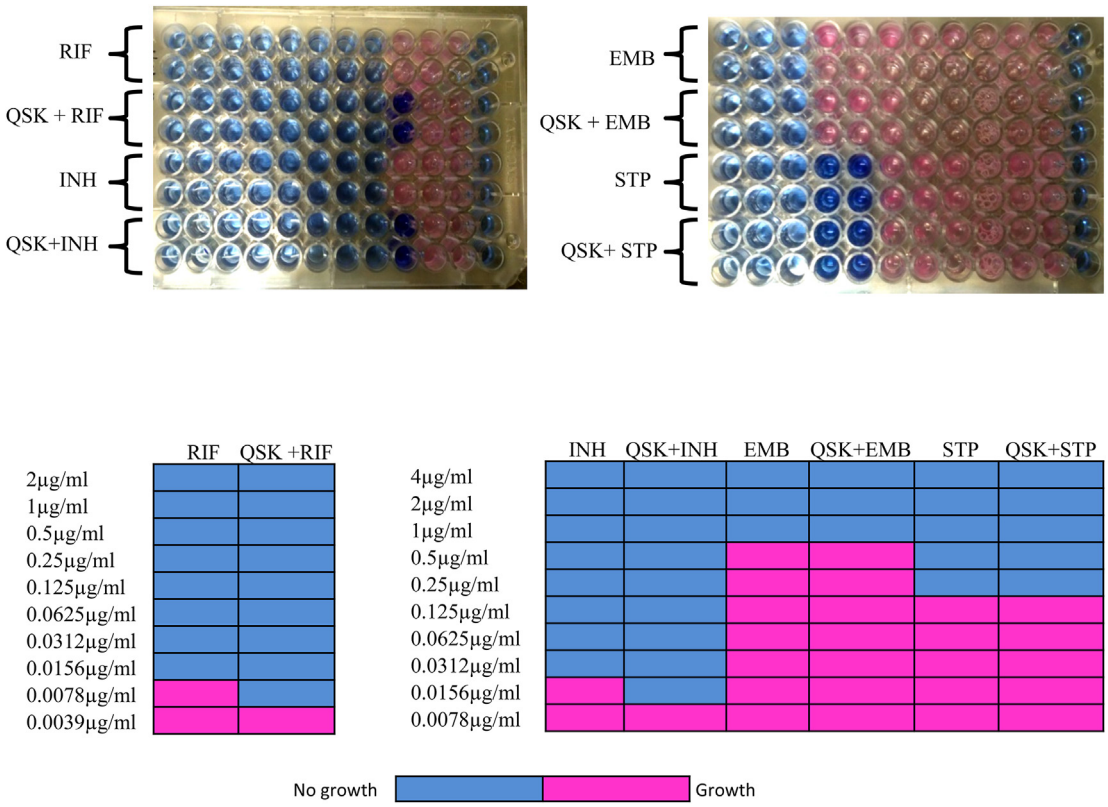

Fig. 1. Effect of QSK on anti-TB drugs susceptibility. The upper panel display MIC of anti-TB drugs (RIF, INH, EMB and STP) and combination with QSK by REMA plate method. The visible color change from blue (resazurin) to pink (resorufin) shows reductive activities of the cells, indicating cell growth. The lower panel represents analogous depiction of broth micro dilution assay of anti-TB drugs concentration and combination with QSK represented by color bars.

3.2. Membrane integrity is disrupted in response to QSK

Firstly, the MTB cells were observed under microscope after ZN staining in presence and absence of QSK, which depicted alteration in cell size and shape (Fig. 2A). The change in the shape of bacteria prompted us to check surface properties of MTB where we studied colony morphology on agar surfaces in the presence of QSK. We observed rough and dry borders of QSK treated colony in comparison to control which showed smooth and waxy borders (Fig. 2B). Furthermore, we checked the cell sedimentation rate which was significantly enhanced in presence of QSK (Fig. 2C). Additionally, we studied membrane permeability of MTB by nitrocefin hydrolysis to determine alteration in membrane integrity. We observed that membrane permeability was considerably enhanced in presence of QSK (Fig. 2D).

3.3. Biofilm formation is inhibited in response to QSK

To study the effect of QSK on biofilm formation, we performed qualitative assay where biofilms were visualized by CV staining. We observed that biofilm formation was considerably inhibited in presence of QSK in comparison to the WT (Fig. 3A). However, QSK had no effect on breaking the mature biofilms (Fig. 3A). We further confirmed quantitatively by estimating the metabolic activity and biomass of biofilms. Both the assays established that metabolic activity and dry weight of biofilm biomass were considerably reduced by 20% (Fig. 3B) and 33% (Fig. 3C) respectively in presence of QSK as compared to control.

3.4. Global lipidome of total lipids in response to QSK

Comparative lipidome profile in response to QSK was performed by mass spectrometry based lipidomics technology as described in methods. We analyzed our LC-MS data with window range (WR) of 0.5 and the data of total lipid analysis revealed that 25 m/z coded for 56 lipids in control whereas 20 m/z coded for 44 lipids when cells are grown in presence of QSK (Fig. S3 A and B). Thus, the output from MS-LAMP obtained upon querying LC-ESI-MS data acquired revealed alteration of lipid profile in presence of QSK. The Venn diagram displayed the number of lipids that were specific and common between control and QSK treated cells. The result of 0.5WR showed, out of 56 lipids, 13 fatty acid (FA), 19 glycerolipids (GL), and 25 glycerophospholipids (GPL) were detected in control while QSK-treated sample revealed 14 FA, 12 GL, 15 GPL and other classes of lipid like polyketide (PK) and saccharolipids (SL) among total 44 lipids (Fig. S3B).

3.5. Alteration of lipid classes in response to QSK

Our lipidomics data revealed that in presence of QSK FA class was affected considerably. We found that the no of *m/z* values corresponding to mycocerosic acid, phthioceranic acid, mycolipenic acid, mycosanoic acid and hydroxythioceranic acid were less (Fig. 4A). Of note, we could detect that specific species of mycocerosic acid (Fig. 4B) and phthioceranic acid (Fig. 4C) were changed. Likewise among another class of lipid namely glycerolipids (GL) we observed lesser *m/z* for monoglycerides (MG), diglycerides (DG) and triglycerides (TG) peaks in presence of QSK (Fig. 5A). This was reflected at the species level of MG (Fig. 5B), DG (Fig. 5C) and TG (Fig. 5D) in response to QSK. Similarly, while analyzing

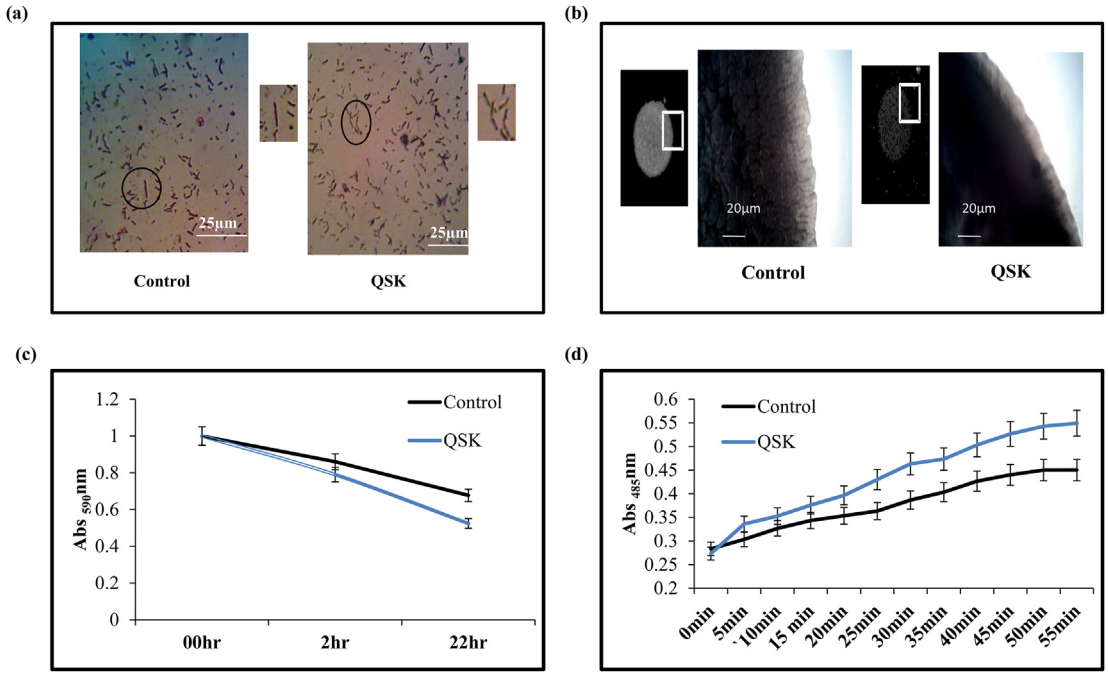

Fig. 2. Effect of QSK on cell surface integrity (A) ZN staining images of control and cells treated with QSK. Scale bar depicts 20 µm. (B) Colony morphology of control and cells treated with QSK observed on 7H10-based medium at 10x magnification. Scale bar depicts 20 µm. (C) Cell sedimentation. Left panel shows $O.D_{600}$ of control cells and treated with QSK depicted on y axis with respect to time (hours) on x-axis. (D) Nitrocefin hydrolysis of control and cells treated with QSK. Mean of $O.D_{485}$ ± SD of three independent sets are depicted on y axis.

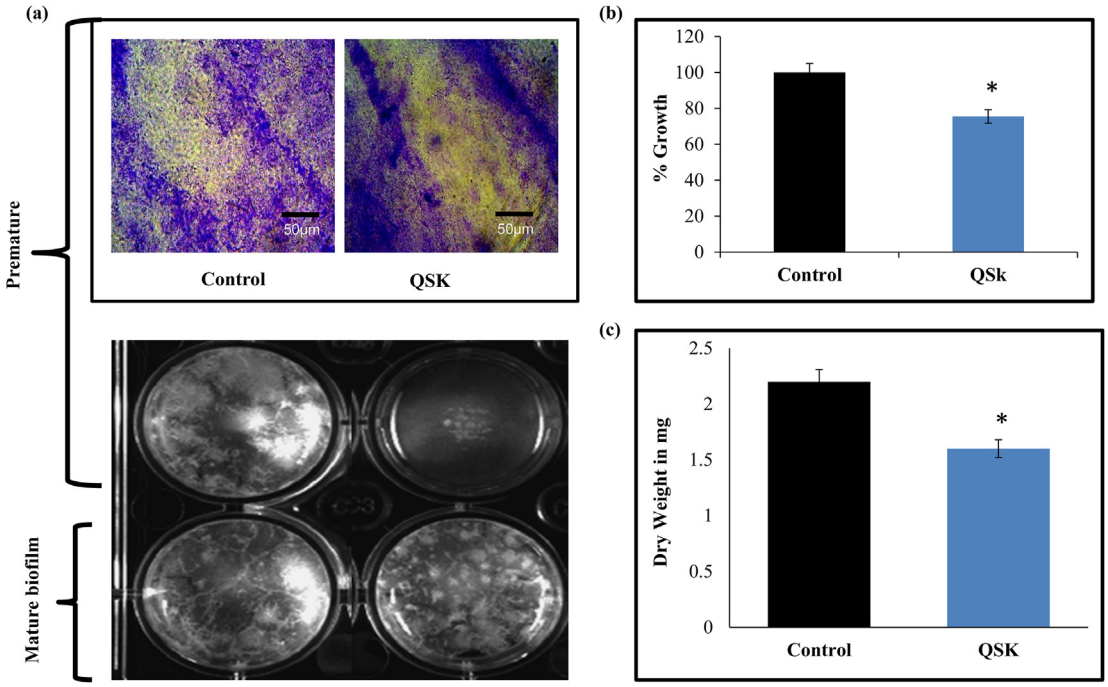

Fig. 3. Effect of QSK on biofilm formation. (A). The upper panel show CV staining depicting biofilm formation in control and in presence of QSK. Scale bar depicts 50 µm. Lower panel depicts bioflim formation on polystyrene surface in presence of QSK. (B) Biofilm metabolic activity (expressed as $O.D_{450}$) depicted as a bar graph. Data are expressed as mean ± SD of three independent sets of experiments and * depicts *P* value < 0.5. (C) Biofilm biomass (dry weight) of control and QSK treated cells. Mean of dry weight ±SD of three independent experiments are depicted on the Y-axis * depicts *P* value < 0.5.

glycerophospholipid (GPL) we observed changes in several sub-classes such as PE, PG, PI, lyso-PG and PIM1 (Fig. 6A).Furthermore at species level we could detect subtle changes in PE (Fig. 6B), lyso-PE (Fig. 6C), PG (Fig. 6D) and lyso-PG (Fig. 6E) levels in response to QSK.

3.6. QSK inhibits MTB growth inside macrophages

The growth of MTB inside macrophage was determined by colony forming unit (CFU). We monitored the CFU counts at different time intervals after infection from 0 till 6 days. The

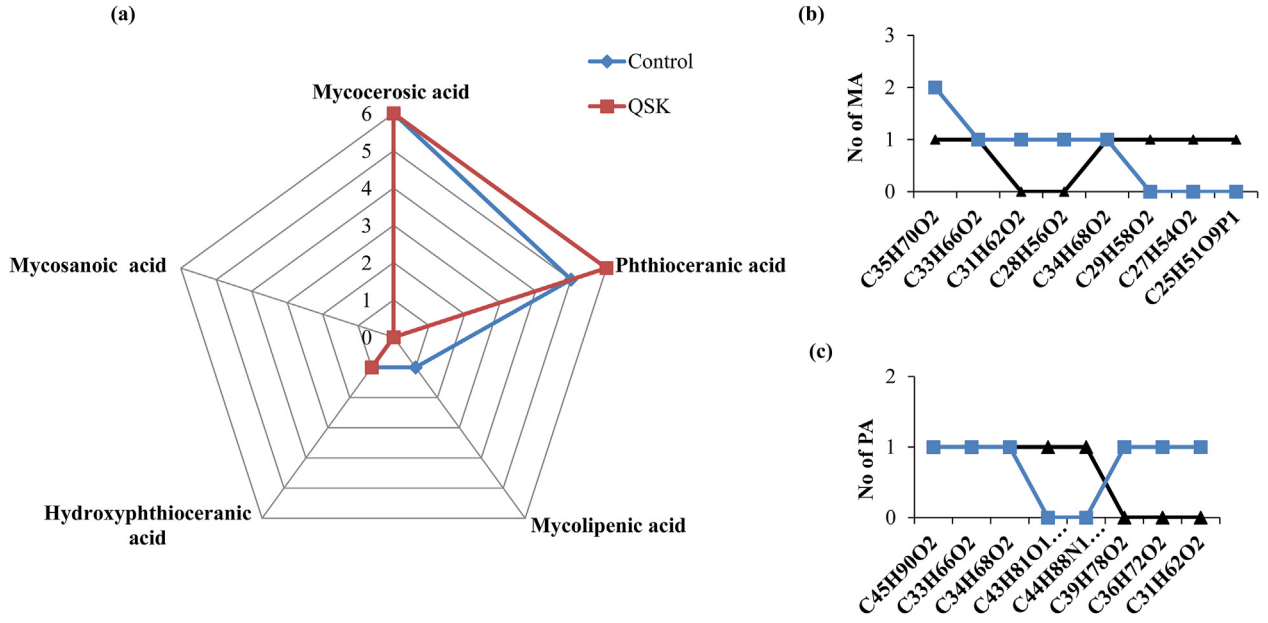

Fig. 4. Changes in FA composition in response to QSK. (A). Web graph depicts number of FA subclasses identified from *m/z* values at WR 0.5 from total lipid through MS-LAMP. (B) Graph represents number of mycocerosic acid and species level changes. (C). Graph represents number of phthioceranic acid and species level changes.

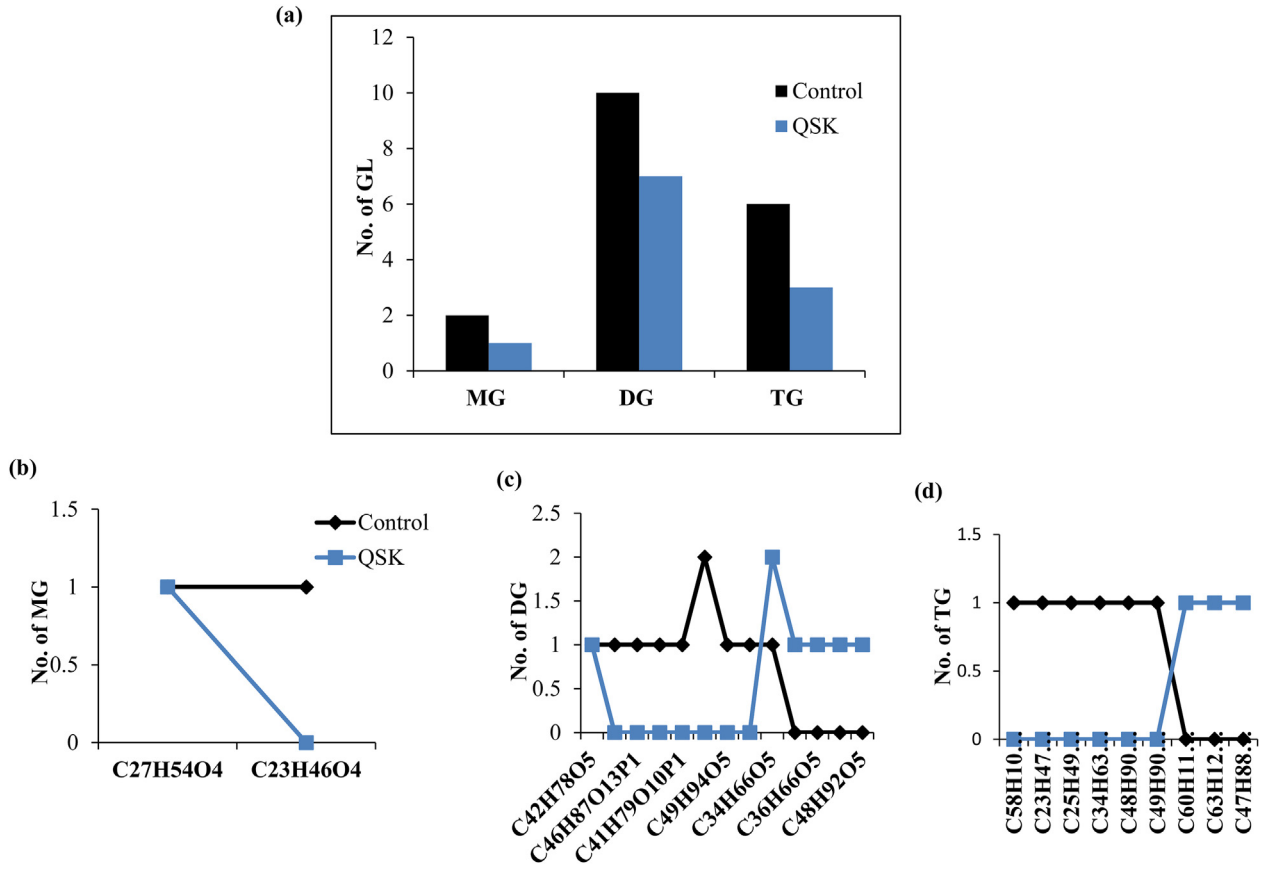

Fig. 5. Changes in GL composition in response to QSK. (A). Bar graph depicts number of GL subclasses (MG, DG and Tg) identified from *m/z* values at WR 0.5 from total lipid through MS-LAMP. (B) Graph represents number of MG and species level changes. (C). Graph represents number of DG and species level changes. (D). Graph represents number of TG and species level changes.

infected THP-1 cell line treated with QSK showed decrease in the bacterial growth at each interval of time. The major difference in total number of bacteria was observed at day 6 in the range of 7.5×10^5 CFU in control contrary to 6×10^5 CFU in presence of QSK

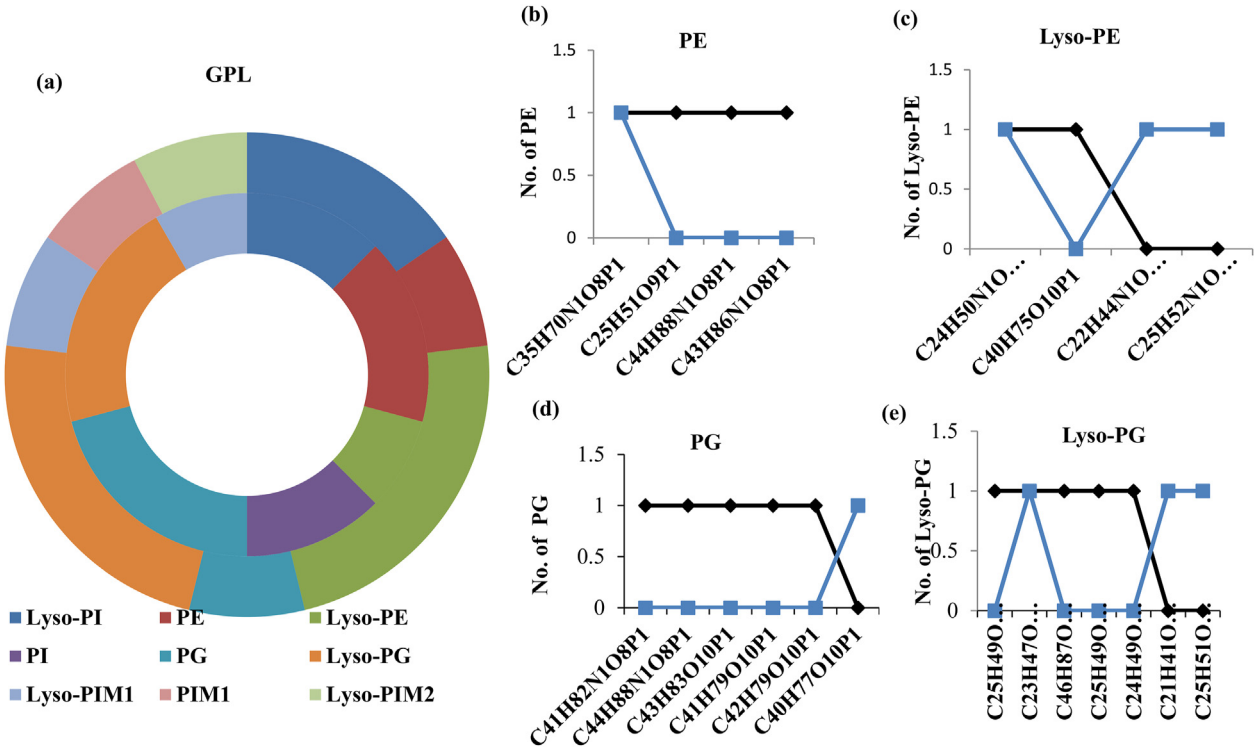

Fig. 6. Changes in GPL composition in response to QSK. (A). Circular graph depicts number of GPL subclasses identified from *m/z* values at WR 0.5 from total lipid through MS-LAMP. Outer circle and inner circle represents control and QSK respectively. (B) Graph represents number of PE and species level changes. (C). Graph represents number of lyso-PE and species level changes. (D). Graph represents number of PG and species level changes. (E). Graph represents number of lyso-PG and species level changes.

(Fig. 7A).

3.7. QSK confers immunomodulatory effect in MTB infected THP-1 cells

Further, we checked the profile of cytokine secretion of THP-1 cells with QSK treated MTB infection. THP-1 cell supernatants were collected at different time points after the infection and cytokine (TNF-alpha, IL-10, IL-6) levels were determined by ELISA. THP-1 infected cell treated with QSK showed enhanced production of proinflammatory cytokines TNF-alpha (Fig. 7B), IL-6 (Fig. 7C) and decrease in anti-inflammatory cytokine IL-10 at different time points (Fig. 7D).

3.8. QSK inhibits intracellular apoptosis of macrophages

Next, we checked the intracellular apoptosis after 6 days of infectivity in THP-1 cells through flow cytometry as described in methods. The apoptosis induced by MTB in THP-1 cells was assessed by Annexin V labeling and Propidium iodide (PI). We observed that infected THP-1 cells treated with QSK induced reduced apoptosis compared to untreated cell (Fig. 8A). Both early (Fig. 8B) and late apoptosis (Fig. 8B) is significantly decreased in presence of QSK.

3.9. Endogenous ROS levels are enhanced in response to QSK

To check the potentiality of the QSK to change the redox status of cells further ROS generation was studied. We examined the generation of ROS in THP-1 infected with MTB and estimated the production of ROS by flow cytometry using 2,79-dichlorofluorescein-diacetate (DCFH-DA) as probe and H_2O_2 as a positive control. The infected THP-1 cell with QSK treated MTB, displayed increase in the ROS generation in comparison to the control (Fig.8C and D).

4. Discussion

With the growing concern of MDR-TBC there is urgent need of alternative therapeutics to reduce the disease burden. Traditional medicines provide one such option that can be exploited to win the battle against TBC.[18] Unani drugs are already in use since ancient times although their mechanism is not well elucidated. This study aimed to enlighten the mechanism of one such anti-TBC unani drug, QSK.

We started our investigation by studying the combinatorial effect of QSK on susceptibilities of known anti-TBC drugs RIF, INH, EMB and STP. Interestingly we could observe that the susceptibility of only RIF and INH were enhanced with no effect on EMB and STP (Fig. 1). Since INH is one of the primary first line anti-TBC drugs that is in use and target MTB membrane, hence we studied the effect of QSK on membrane more closely. Altered cell sizes depicted by ZN staining (Fig. 2A), changes in morphology of bacteria (Fig. 2B) and cell sedimentation rate (Fig. 2C) in presence of QSK reinforce the fact of disrupted cell membrane homeostasis. This result further encourages us to perform membrane permeability assays using nitrocefin which is a chromogenic cephalosporin substrate containing an amide bond in the β-lactam ring, hydrolyzed by β-lactamase enzyme, normally localized to the bacterial periplasm. Thus increased hydrolysis determines the increased membrane permeability which we found to be considerably enhanced in presence of QSK (Fig. 2D).

Formation of biofilm is one of the major contributor in virulence and drug resistance in mycobacteria.[19] Biofilm are extremely resistance to anti-TBC drug during infection and display reduced susceptibility to alter the host immune response.[20] Biofilms are

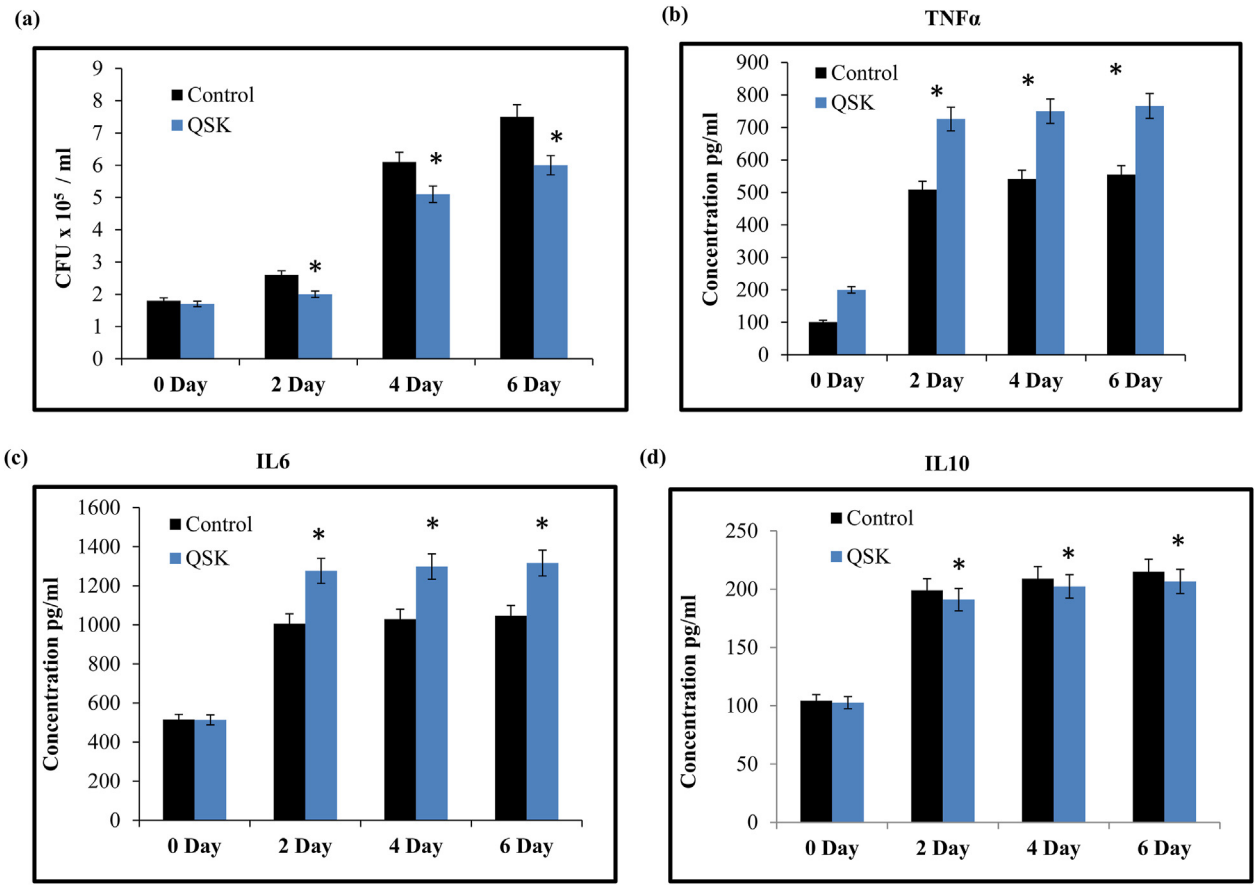

Fig. 7. Intracellular growth of MTB and Cytokine profiling in presence of QSK. (A) Bar graph represents CFU/ml on y-axis with respect to number of days on x-axis. THP-1 cells were infected with MTB at MOI of 10 for 0, 2, 4, 6 days. After each incubation time, the infected cells were lysed and colonies were counted after 30 days of plating. Three such independent experiments were carried out and the data points represent mean of all three experiments. (B–D) Bar graph represents cytokine levels measured in pg/ml on y-axis with respect to time on x-axis. Cells were infected with MTB at a MOI of 10, and supernatants were collected at different time points after infection and analyzed with specific ELISA for proinflammatory cytokines (B) TNF-α (C) IL-6 (D) IL-10. The results represent the means of three separate experiments, * depicts *P* value < 0.5.

formed by the adhesion of bacterial cells to the cell surface through extracellular polymeric substances. Further, examination of biofilm formation revealed that QSK treatment inhibits biofilm formation (Fig. 3A). Quantitative assay of biofilm formation by crystal violet, a dye to stain bacterial peptidoglycan layer reveals 20% inhibition in biofilm formation (Fig. 3B). When dry weight of the cells in biofilm was measured it was found to be decreased by 33% in presence of QSK (Fig. 3C). These results confirmed that QSK is a potent inhibitor of virulence attributes associated with MTB, resulting in inhibition of biofilm formation.

MTB has distinctive cell-surface architectures comprised of mycolic acid (MA) residues which are hallmark features.[21] The MA is the most essential component of mycobacterial cell wall and striking target of numerous anti-TBC drugs.[22] Several observations from this study such as enhanced INH susceptibility, altered membrane integrity and inhibited biofilm formation led us to explore the changes associated with cell envelope intricately. Hence, we performed mass spectrometry based lipidomics to comprehend the changes in response to QSK. The mycobacterial cell wall is composed of complex lipids that are important for pathogenesis.[23] The biosynthesis of FA plays a vital role in the formation of cell wall components, particularly MA which is required for the survival of MTB in the host.[24] Mycolipenic acids are trimethyl branched FA present in the polyacrylate trehalose (PAT), and are synthesized on the periplasmic side of the membrane and then transported to the outer membrane of *Mycobacterium* that plays a structural role in the cell envelope as well as modulating host immune responses.[25] In our study we found inhibition of mycolipenic acid which also supported our above result that QSK affects the cell membrane of the mycobacteria (Fig. 4).

GL is another class of lipids with three subclasses namely MG, DG and TG. TG is the primary form of storage lipid-based energy reserves in *Mycobacterium* which is catabolized by lipase enzymes in stressed condition and play a vital role in pathogenesis.[10,26] Our result showed less *m/z* values corresponding for MG leading to further decrement in DG and TG expressions (Fig. 5). Phosphatidylethanolamine (PE), phosphatidylinositol (PI), phosphatidylglycerol (PG), phosphatidylserine (PS), cardiolipin (CL), and mannosylated forms of PI known collectively as PIMs are the major structural lipid constituents of the plasma membrane of MTB.[27] PG involved in synthesis of CL is one of the abundant phospholipids in mycobacteria and form aggregates within membrane bilayer. PE is the structural component of plasma membrane whereas PI is the important class of phospholipids that are known to be further modified by extensive glycosylation (PIM, LM, and LAM).[12] PIM plays a crucial role in permeability of cell envelope, regulation of cell septation and division and maintain the inner membrane integrit[y11]. In our study we found less *m/z* values corresponding for PE, PI and PG which reinforce global lipid remodeling in response to QSK (Fig. 6).

Pathogenesis in TBC is also governed by various factors driven by the host immune system. In the present study, innate responses in

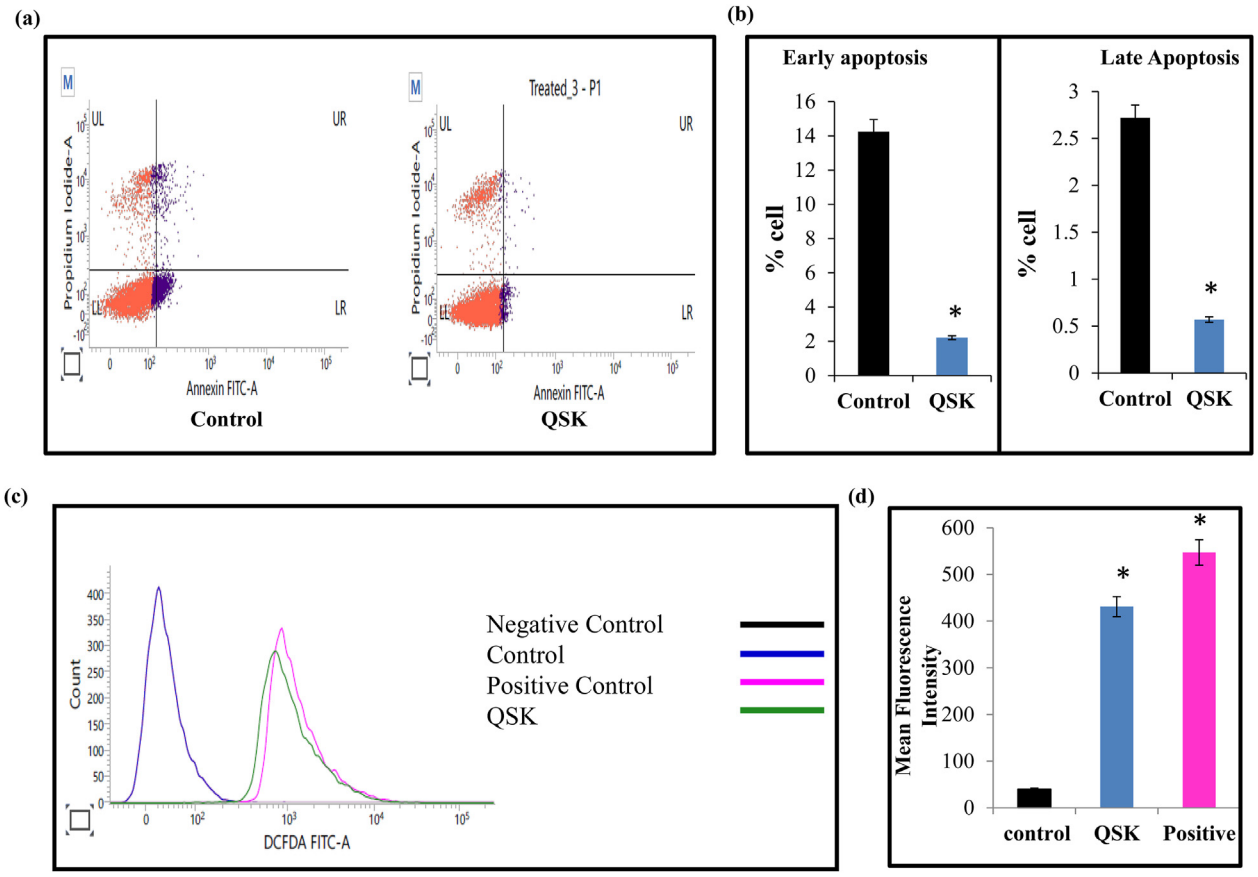

Fig. 8. Effect of QSK on apoptosis and ROS production. (A). Flow-cytometry analysis of Annexin V–positive cells, uninfected THP-1 cell and MTB infected THP-1 in the presence and absence of QSK. (B) The bar graph represents percentage of Annexin V or propidium iodide–positive cells for early and late apoptosis respectively. (C) Effect of QSK on intracellular ROS generation with DCFDA observed by using flowcytometer. Annexin V-FITC staining Mtb-infected (blue overlay) THP-1 cells and QSK treated showed green overlay.(D) Bar graph represents mean fluorescence intensity on y-axis with respect to control, QSK and hydrogen peroxide (positive control).

presence of QSK were relatively evaluated in terms of intracellular growth, cytokine profiling and induction of apoptosis and ROS. The intracellular growth of MTB inside THP-1 cells was considerably decreased in the presence of QSK as estimated by CFU (Fig. 7A). The intracellular MTB growth is an indicator of virulence and infact a study has suggested that virulent strains grew faster than the non-virulent strains.[28] The production of proinflammatory cytokines is essential for host resistance against MTB infection and dictates the intracellular survival. TNF-α production is an important early event that leads to granuloma formation and a protective host immune response.[29] Similarly, IL-6 has also been recommended to be an essential proinflammatory cytokine during acute infection.[30] In our study we observed that both proinflammatory cytokines TNF- α and IL-6 were enhanced in presence of QSK (Fig. 7B and C) which is important for innate and protective immunity against MTB. Contrary, MTB infected macrophages produce the immunosuppressive cytokine IL-10. It is possible that elevated IL-10 production levels in MTB infected THP-1 cell plays an anti-inflammatory role through the inhibition of IL-12 expression.[31,32] We observed that IL-10 level was decreased in the presence of QSK (Fig. 7D).

MTB infection in macrophages and generation of proinflammatory cytokines are known to induce apoptosis.[16] Hence we studied the early and late apoptosis in response to QSK. We explored that both the early and late apoptosis were inhibited in response to QSK (Fig. 8A and B). MTB utilizes a variety of pathways to protect against ROS from direct scavenging of the reactive species and the DNA repair and protection of proteins.[33] To gain further insights into the anti-TB effect of QSK, ROS generation was estimated in MTB infected THP-1 cells. Our result suggested increase in ROS production in presence of QSK as revealed by flow cytometric analysis of ROS positive cells after infection comparable to positive control hydrogen peroxide (Fig. 8C and D). ROS formation can lead to the development of chemical reactions causing damage to cellular components, including nucleic acids, proteins and lipids.[33]

5. Conclusion

The present study uncovers the diverse targets of unani anti-TBC drug, QSK and endorse that traditional medicine represents an untapped resource for development of new anti-TB drugs. The combinatorial effect of QSK along with anti-TBC drugs may be adopted as strategy to control TBC.

Declaration of competing interest

The authors declare that there are no competing interests.

Acknowledgement

Financial assistance to Z.F from Ministry of AYUSH, New Delhi (Z.28015/227/2015-HPC (EMR)-AYUSH C) is deeply acknowledged. We thank Unani expert, Dr. Nafia Jeelani for her support in procurement and standardization of QSK drug concentration for experiments. We are grateful to Dr. Mandira Varma-Basil and Dr.

Ramandeep Singh, for providing MTB $H_{37}R_v$ strain and THP-1 cell lines as generous gifts respectively. We thank Amity Lipidomics Research Facility (ALRF) and Central Instrumentation Research Facility (CIRF), Amity University Haryana for facilitating us in mass spectrometry and flowcytometry experiments respectively. We also thank Padma Shri Dr. M. A. Waheed from CCRUM, New Delhi for encouragement.

Appendix A. Supplementary data

Supplementary data to this article can be found online at https://doi.org/10.1016/j.jtcme.2021.07.009.

References

1. Zaman K. Tuberculosis: a global health proble. *J Health Popul Nutr*. 2010;28:111–113.
2. World health organization reports. https://www.who.int/publications/i/item/9789240013131; 2020.
3. World Health Organization reports. https://www.who.int/teams/global-tuberculosis- programme/tb-reports; 2020.
4. Mello FCQ, Silva DR, Dalcolmo MP. Tuberculosis: where are we? *J Bras Pneumol*. 2018;44:82 (d).
5. Chatterjee S, Poonawala H, Jain Y. Drug-resistant tuberculosis: is India ready for the challenge? *BMJ Glob Health*. 2018;3, e000971.
6. Jamil S, Jabeen A, Ahmad S. *Pulmonary tuberculosis and its management in classical Unani literature*. 2005;4:143–149.
7. Quddus A, Siddiqui MMH, Siddiqui MY, et al. Clinical evaluation of the efficacy of Qurs Sartan Kafoori and Sharbat Zoofa Murakkab in chronic bronchitis. 2009;8:417–420.
8. Kabiruddin M. *Bayaz Kabir, Delhi Ka Matab*. vol. I. Gujrat: Shaukat Book Depot, Shaukat Bazar; 1935:15–22.
9. Hans S, Sharma S, Hameed S. Sesamol exhibits potent antimycobacterial activity: underlying mechanisms and impact on virulence traits. *J Glob Antimicrob Resist*. 2017;10:228–237.
10. Pal R, Hameed S, Kumar P, Singh S, Fatima Z. Understanding lipidomic basis of iron limitation induced chemosensitization of drug resistant. *Mycobacterium tuberculosis. 3 Biotech*. 2019;9:122.
11. Pal R, Hameed H, Sharma S, Fatima Z. Influence of iron deprivation on virulence traits of mycobacteria. *Braz J Infect Dis*. 2016;20:585–591.
12. Sharma S, Hameed S, Fatima Z. Lipidomic insights to understand membrane dynamics in response to vanillin in Mycobacterium smegmatis. *Int Microbiol*. 2020;23:263–276.
13. Sabareesh V, Singh G. Mass spectrometry based lipid(ome) analyzer and molecular platform: a new software to interpret and analyze electrospray and/or matrix-assisted laser desorption/ionization mass spectrometric data of lipids: a case study from Mycobacterium tuberculosis. *J Mass Spectrom*. 2013;48:465–477.
14. Sartain MJ, Dick DL, Rithner CD, et al. Lipidomic analyses of Mycobacterium tuberculosis based on accurate mass measurements and the novel BMtb Lipid DB. *J Lipid Res*. 2011;52:861–872.
15. Arora G, Chaudhary D, Kidwai S, et al. CitE enzymes are essential for Mycobacterium tuberculosis to establish infection in macrophages and Guinea pigs. *Front Cell Infect Microbiol*. 2018;8:385.
16. Chakraborty P, Kulkarni S, Rajan R, et al. Drug resistant clinical isolates of Mycobacterium tuberculosis from different genotypes exhibit differential host responses in THP-1 cells. *PloS One*. 2013;8, e62966.
17. Shin DM, Jeon BY, Lee HM, et al. Mycobacterium tuberculosis eis regulates Autophagy,Inflammation, and cell death through redox-dependent Signaling. *PLoS Pathog*. 2010;6, e1001230.
18. Sharma P, Verma M, Bhilwar M, et al. Epidemiological profile of tuberculosis patients in Delhi, India: a retrospective data analysis from the directly observed treatment short-course (DOTS) center. 2019;8:3388–3392.
19. Sharma D, Misba L, Khan AU. Antibiotics versus biofilm: an emerging battleground in microbial communities. *Antimicrob Resist Infect Contr*. 2019;8:76.
20. Singh S, Singh SK, Chowdhury I, et al. Understanding the mechanism of bacterial biofilms resistance to antimicrobial agents. *Open Microbiol J*. 2017;11:53–62.
21. Abrahams KA, Besra GS. Mycobacterial cell wall biosynthesis: a multifaceted antibiotic target. *Parasitology*. 2018;145:116–133.
22. Vilchèze C. Mycobacterial cell wall: a source of successful targets for old and new drugs. *Appl Sci*. 2020;10:2278.
23. Ghazaei C. Mycobacterium tuberculosis and lipids: insights into molecular mechanisms from persistence to virulence. *J Res Med Sci*. 2018;23:63.
24. Kinsella RJ, Fitzpatrick DA, Creevey CJ, et al. Fatty acid biosynthesis in Mycobacterium tuberculosis: lateral gene transfer, adaptive evolution, and gene duplication. *Proc Natl Acad Sci U S A*. 2003;100:10320–10325.
25. Belardinelli JM, Larrouy-Maumus G, Jones V, et al. Biosynthesis and translocation of unsulfated acyltrehaloses in Mycobacterium tuberculosis. *J Biol Chem*. 2014;289:27952–27965.
26. Deb C, Daniel J, Sirakova TD, et al. A novel lipase belonging to the hormone-sensitive lipase family induced under starvation to utilize stored triacylglycerol in Mycobacterium tuberculosis. *J Biol Chem*. 2006;281:3866–3875.
27. Jackson M. The mycobacterial cell envelope-lipids. *Cold Spring Harb Perspect Med*. 2014;4:a02110.
28. Chai Q, Wang L, Liu CH, et al. New insights into the evasion of host innate immunity by Mycobacterium tuberculosis. *Cell Mol Immunol*. 2020;17:901–913.
29. Sasindran SJ, Torrelles JB. Mycobacterium tuberculosis infection and inflammation: what is beneficial for the host and for the bacterium? *Front Microbiol*. 2011;2:2.
30. Tanaka T, Narazaki M, Kishimoto T. IL-6 in inflammation, immunity, and disease. *Cold Spring Harb Perspect Biol*. 2014;6:a016295.
31. D'Andrea AM. Aste-Amezaga NM, Valiante XMa et al. Interleukin 10 (IL-10) inhibits human lymphocyte interferon g-production by suppressing natural killer cell stimulatory factor/IL-12 synthesis in accessory cells. *J Exp Med*. 1993;178:1041.
32. Isler P, Rochemonteix BGd, F Songeon N, et al. Interleukin-12 production by human alveolar macrophages is controlled by the autocrine production of IL-10. *Am. J. Resp. Cell Mol.* 1999;20:270.
33. Nita M, Grzybowski A. The role of the reactive oxygen species and oxidative stress in the pathomechanism of the age-related ocular diseases and other pathologies of the anterior and posterior eye Segments in adults. *Oxid Med Cell Longev*. 2016;2016:3164734.